

## HOMOGENEITY OF STELLAR POPULATIONS IN EARLY-TYPE GALAXIES WITH DIFFERENT X-RAY PROPERTIES

TADAYUKI KODAMA<sup>1,2</sup> & KYOKO MATSUSHITA<sup>3</sup>

1) Department of Physics, University of Durham, South Road, Durham DH1 3LE, UK

2) Department of Astronomy, University of Tokyo, Hongo, Bunkyo-ku, Tokyo 113-0033, Japan

3) Department of Physics, Tokyo Metropolitan University, 1-1 Minami-Ohsawa Hachioji, Tokyo 192-0397, Japan

*Received — ; Accepted —*

### ABSTRACT

We have found the stellar populations of early-type galaxies are homogeneous with no significant difference in color or Mg2 index, despite the dichotomy between X-ray extended early-type galaxies and X-ray compact ones. Since the X-ray properties reflect the potential gravitational structure and hence the process of galaxy formation, the homogeneity of the stellar populations implies that the formation of stars in early-type galaxies predates the epoch when the dichotomy of the potential structure was established.

*Subject headings:* galaxies: elliptical and lenticular — galaxies: formation — galaxies: evolution — galaxies: stellar content — galaxies: ISM

### 1. INTRODUCTION

ASCA X-ray observations of NGC 4636 (Matsushita et al. 1998) and some other giant early-type galaxies (Matsushita 1997) show that early-type galaxies can be classified into two categories in terms of X-ray extent. Some early-type galaxies have a very extended dark matter halo characterized by X-ray emission out to  $\sim 100$  kpc from the galaxy center, while others have a compact X-ray halo. The galaxies with an extended X-ray emission can be interpreted as sitting in larger scale potential structure, such as galaxy groups, subclumps of clusters, or clusters themselves, as well as sitting their own potential well associated with each galaxy.

Potential structure must have played a big role in the course of galaxy formation. If the difference in potential structure had been already established before the bulk of stars formed, we would expect some differences in stellar populations, such as mean age or metallicity, as well. A deeper potential well would keep the gas more effectively against the thermal energy input by supernova (SN) explosion, and the chemically enriched gas can be recycled more efficiently, and the galaxy would end up with higher mean stellar metallicity (Larson 1974). Therefore we would expect that the X-ray extended galaxies have higher metallicities than the X-ray compact ones at a given stellar mass. Furthermore, considering that the higher density peaks collapse earlier in the Universe, which is likely to be the case for the X-ray extended galaxies sitting in the local density peaks, we would also expect their older ages than those of the X-ray compact ones. Both of these effects would make the colors of the X-ray extended galaxies redder. The central question of this paper is, therefore, how this dichotomy in X-ray properties hence the potential structure is related to the optical properties which trace the stellar populations in galaxies.

Another interesting issue is whether the number of globular clusters per unit optical luminosity of galaxy correlates with the X-ray extent of galaxy. This is because, if the X-ray extended galaxies are the products of galaxy mergers as they are located in the center of larger scale potential structure, and if a considerable number of new globular clusters form during galaxy mergers as suggested by Zepf and Ashman (1993), we would expect more globular clusters in the X-ray extended galaxies for a given optical luminosity.

Matsushita (2000; hereafter M2000) has recently compiled the X-ray properties of 52 nearby early-type galaxies from ROSAT data. Together with the archival data of various optical properties, we now compare the optical properties with the X-ray properties to examine the correlation between them.

The structure of this paper is the following. In § 2 we summarize the X-ray properties of our sample of early-type galaxies, highlighting the dichotomy of the potential structure. In § 3 we present their optical properties, including integrated colors and Mg<sub>2</sub> index. We show the homogeneity of the stellar populations despite the dichotomy in X-ray properties. We discuss the impact of this result on the formation of early-type galaxies in § 4, and conclude the paper in § 5. We use  $H_0 = 75 \text{ km s}^{-1} \text{ Mpc}^{-1}$  throughout this paper.

### 2. X-RAY PROPERTIES

We use the same sample of early-type galaxies presented in M2000. The sample is composed of 52 bright early-type galaxies, of which 42 are ellipticals and 10 are S0 galaxies. M2000 have selected all the early-types observed by PSPC, available in the ROSAT archival data, whose *B*-band magnitudes are brighter than 11.7. The environment of the sampled galaxies varies from cluster environment (Virgo, Fornax, and Centaurus clusters) to galaxy groups and the field.

Figure 1 shows X-ray luminosity of the inter stellar medium (ISM) within a radius of  $4r_e$  ( $L_X$ ) against  $L_B\sigma^2$  for all the sample galaxies, where  $r_e$ ,  $L_B$  and  $\sigma$  indicate the effective radius in the optical profile, the galaxy luminosity in *B*-band (taken from Tully 1988), and the central velocity dispersion of stars, respectively. In order to exclude the contribution from low mass X-ray binaries and the active galactic nuclei, the ROSAT PSPC spectrum (0.2-2.0 keV) is fitted with two components; soft ( $\sim 1$  keV) and hard (10 keV), and only the soft component is used to determine the ISM X-ray luminosity (M2000). The quantity  $L_B\sigma^2$  is proportional to the kinetic energy of the gas supplied from stellar mass loss and heated up by random stellar motions. The solid line,  $\log L_X/(L_B\sigma^2)=25.15$  (const), corresponds to the energy balance between the cooling by X-ray emission and the heating by stellar mass loss, assuming a relation between mass loss rate and  $L_B$  (Ciotti et al. 1991; M2000). There is a considerable scatter in  $L_X$  for a given  $L_B\sigma^2$ .

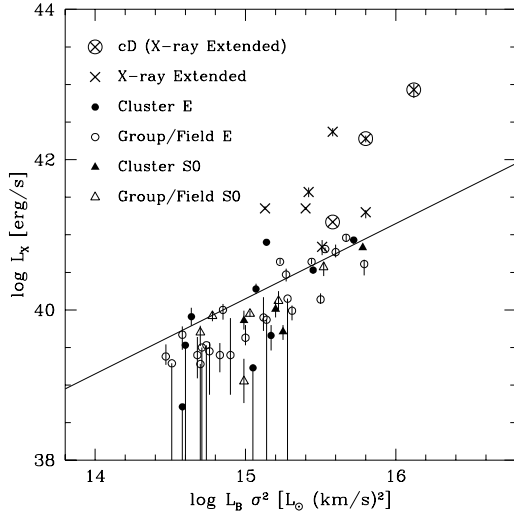


Fig. 1. X-ray luminosity ( $L_X$ ) within  $4r_e$  versus  $L_B\sigma^2$ . Vertical error bars show two sigma errors in  $L_X$ . Crosses indicate the X-ray extended galaxies, and those surrounded by big circles are the cD galaxies. The galaxies in cluster environment are shown by filled symbols, while those in the field or in small groups are shown by open symbols. Ellipticals are indicated by circles, while S0's are indicated by triangles. The solid line corresponds to  $\log L_X / (L_B\sigma^2) = 25.15$  (constant), on which the X-ray luminosity is just comparable to the kinetic energy input to the ISM by stellar mass loss and the heating of the ejected gas by random stellar motions.

Many galaxies follow the solid line, suggesting that their X-ray luminosities can be simply explained by the energy input from stars through mass loss. However some galaxies have significantly higher  $L_X/L_B\sigma^2$  ratios, requiring an excess energy to explain such high X-ray luminosities. Many of these  $L_X$  bright galaxies are classified as X-ray extended galaxies in M2000 (crosses) as they show spatially extended X-ray emission. They are likely to have more extended dark matter halos residing on larger scale structure, such as a group or a cluster of galaxies, as well as on its own galaxy. Furthermore, the X-ray extended galaxies show significantly higher ISM temperatures at  $r > r_e$  than that of the X-ray compact ones as a result of their extended potential. In fact, their mean ISM temperature within  $4r_e$  is about factor of 2 higher than the others at a given  $\sigma$  (M2000). We reproduce this plot in Fig. 2. We refer these differences as a dichotomy of X-ray properties. Therefore we will use a quantity  $E_X = \log L_X / (L_B\sigma^2) - 25.15$ , the excess energy in  $L_X$ , as a measure of the ‘X-ray extent’ later in § 3. Larger  $E_X$  means that a galaxy has a deeper and more extended potential. The galaxies which are classified as X-ray extended ones in M2000 are the following nine: NGC 4406 (bright galaxy in Virgo cluster), NGC 4472 (brightest galaxy in Virgo), NGC 4486 (cD in Virgo), NGC 4636 (bright galaxy in Virgo), NGC 4696 (cD in Centaurus cluster), NGC 1399 (cD in Fornax cluster), NGC 1407 (group center), NGC 5044 (group center), and NGC 5846 (group center).

### 3. OPTICAL PROPERTIES

We have compiled the optical properties of our sample galaxies from various sources. The integrated colors are taken from de Vaucouleurs et al. (1991; RC3). Following Schweizer & Seitzer (1992), we defined  $(U-V)_{e,0}$  as

$$(U-V)_{e,0} = (U-V)_e + [(U-V)_{T,0} - (U-V)_T], \quad (1)$$

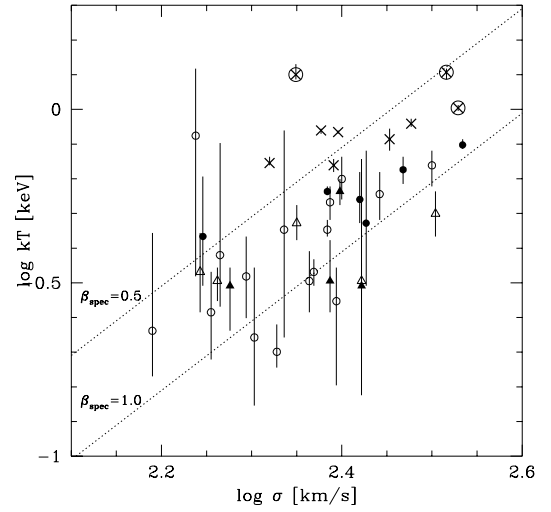


Fig. 2. The ISM temperature ( $kT$ ) within  $4r_e$  versus central stellar velocity dispersion ( $\sigma$ ). Crosses indicate the X-ray extended galaxies, and those surrounded by big circles are the cD galaxies. The galaxies in cluster environment are shown by filled symbols, while those in the field or in small groups are shown by open symbols. Ellipticals are indicated by circles, while S0's are indicated by triangles. Two dotted lines correspond to  $\beta_{\text{spec}}=0.5$  (upper) and  $\beta_{\text{spec}}=1.0$  (lower), respectively, where  $\beta_{\text{spec}}$  is the ratio between kinetic temperature of stars and the gas temperature.

where subscript  $T$  denotes global colors, subscript 0 indicates colors corrected for Galactic extinction and redshift, and subscript  $e$  denotes average colors within the effective radius ( $r_e$ ).  $(B-V)_{e,0}$  is also defined in a similar way. The integrated colors within  $r_e$  in the Cousins system,  $(V-R)_e$  and  $(V-I)_e$ , are taken from Buta & Williams (1995). Galactic extinction is corrected for using the extinction in  $B$ -band ( $A_B$ ) from RC3 and the extinction curve from Rieke & Lebofsky (1985). The reddening corrected colors are denoted as  $(V-R)_{e,0}$  and  $(V-I)_{e,0}$ . The reason why we use colors within  $r_e$  rather than the total colors is that there are more galaxies available with  $r_e$  apertures. This improves the statistics. Furthermore, the colors within  $r_e$  would be more reliable than the total colors, although no errors are given in the literature for the total colors. However, we have checked that the results in this paper did not change even if we used the total colors. The central line index  $\text{Mg}_2$ , central velocity dispersion ( $\sigma$ ), maximum rotation velocity ( $V_m$ ), and deviation from the Fundamental Plane ( $\Delta\text{FP}$ ) are obtained from Prugniel & Simien (1996). A velocity dispersion for NGC 4696 is added from Faber et al. (1989). The globular cluster specific frequency ( $S_N$ ), which is the number of globular clusters per unit galaxy luminosity, is acquired from Ashman & Zepf (1998). Finally, the  $a_4$  index, which is the fourth cosine coefficient of the Fourier expansion of isophotal deviation from a pure ellipse, and the ellipticity ( $\epsilon$ ) are taken from Bender et al. (1989). We will use these values later in this section. The number of galaxies which have optical properties available are 44 ( $U-V$ ), 47 ( $B-V$ ), 32 ( $V-R$ ), 32 ( $V-I$ ), 43 ( $\text{Mg}_2$ ), 49 ( $\Delta\text{FP}$ ), 44 ( $V_m$ ), 23 ( $S_N$ ), and 25 ( $a_4$ ) out of a total of 52 galaxies in our X-ray sample.

In the top three panels of Fig. 3, we have plotted  $U-V$ ,  $V-I$  colors and  $\text{Mg}_2$  index against  $\log \sigma$ . The error-bars indicate one sigma measurement errors. The error-bars are not shown for  $\text{Mg}_2$ , but are negligibly small ( $<0.005$ ). The typical error for  $\log \sigma$  is  $\sim 0.02$  (Prugniel & Simien 1996). We find the scaling

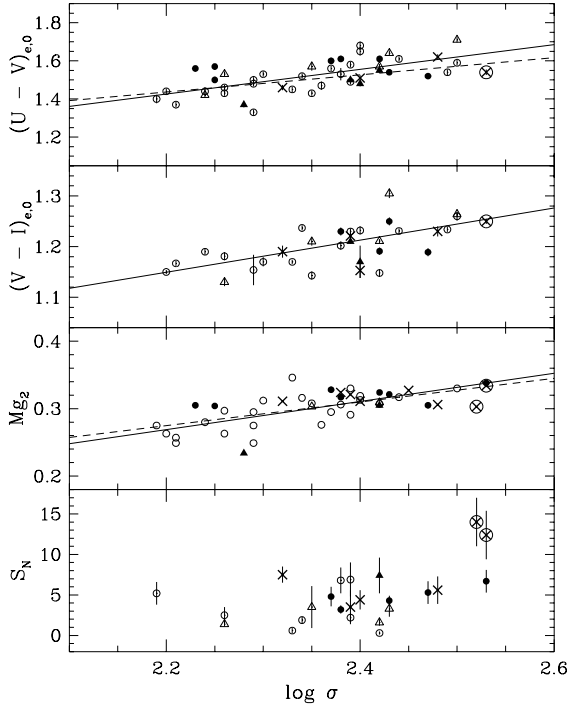


Fig. 3. Integrated colors within an effective radius  $(U - V)_{e,0}$  and  $(V - I)_{e,0}$ , central  $Mg_2$  index, and globular cluster specific frequency  $S_N$  (from top to bottom) are plotted against the central stellar velocity dispersion  $\sigma$ . Vertical error-bars (one sigma) are shown except for the  $Mg_2$  index. Crosses indicate the X-ray extended galaxies, and those surrounded by big circles are the cD galaxies. The galaxies in cluster environment are shown by filled symbols, while those in the field or in small groups are shown by open symbols. Ellipticals are indicated by circles, while S0's are indicated by triangles. The solid lines are the linear regression lines fitted to the data excluding the X-ray extended galaxies. The dashed lines show the relations taken from the literature (Bower et al. 1992; Burstein et al. 1988).

relations for the early-type galaxies as a whole which are shown by the solid lines. The linear regression lines are fitted to the data excluding the X-ray extended galaxies in order to see the difference between the X-ray extended galaxies (crosses) and the X-ray compact ones (the others), if present. For comparison, the same relations taken from Bower, Lucey & Ellis (1992) and Burstein et al. (1988) are also reproduced by the dashed lines on the top panel and the third one, respectively. Our regression lines agree very well with those in the literature. Most important, none of the  $U - V$ ,  $V - I$ , and  $Mg_2$  indices of the X-ray extended galaxies looks different from that of the X-ray compact ones, being well within the scatter at fixed  $\sigma$ .

$S_N$  is plotted against  $\log \sigma$  in the bottom panel of Fig. 3. The error-bars correspond to one sigma. Again, the X-ray extended galaxies do not have systematically different  $S_N$  values, except the two circled galaxies, NGC 1399 and NGC 4486 (the former has a larger  $\sigma$ ), which have a factor of 2-3 as many globular clusters for a given optical galaxy luminosity. These are both cD galaxies in nearby clusters which might have had rather different mechanism of globular cluster formation, such as secondary formation in the cooling flows (Richer et al. 1993, but see also Holtzman et al. 1996 for an objection), capture of globular clusters from other galaxies through tidal stripping (Côté, Marzke & West 1998) or the debris of cannibalized nucleated dwarf galaxies (Bassino, Muzzio & Rabolli 1994). Apart from

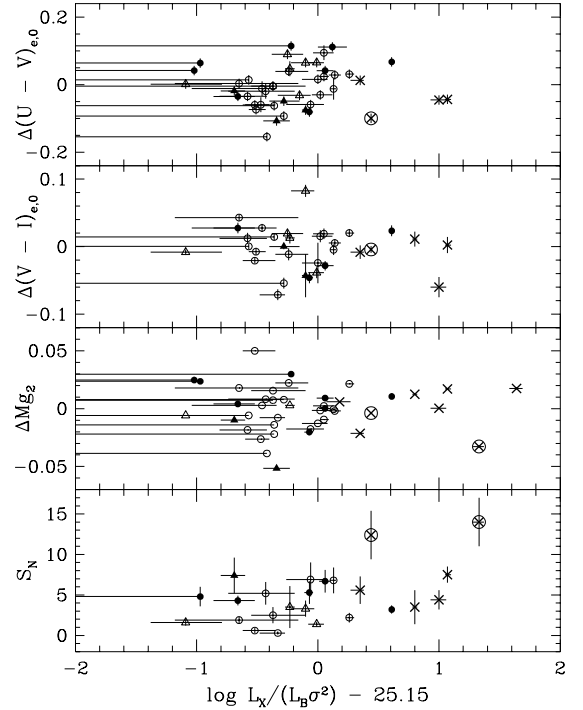


Fig. 4. Deviations from the  $(U - V) - \sigma$  and  $(V - I) - \sigma$  relations, deviation from the  $Mg_2 - \sigma$  relation, and  $S_N$  (from top to bottom) are plotted against the X-ray extent defined as  $E_X = \log L_X / (L_B \sigma^2) - 25.15$ . Vertical error-bars (one sigma) are shown except for the  $Mg_2$  index, and the horizontal error-bars correspond to two sigma errors in  $L_X$ . Crosses indicate the X-ray extended galaxies, and those surrounded by big circles are the cD galaxies. The galaxies in cluster environment are shown by filled symbols, while those in the field or in small groups are shown by open symbols. Ellipticals are indicated by circles, while S0's are indicated by triangles.

these cD galaxies, the number of globular clusters seems comparable between the X-ray extended galaxies and the X-ray compact ones. The consequence of this result will be discussed in § 4.

In order to compare the optical properties against the X-ray properties in a more general manner, we use  $E_X$  as a measure of the X-ray extent or the depth of the potential (§ 2). To subtract the underlying metallicity effect as a function of galaxy mass (or  $\sigma$ ) which is present in early-type galaxies (eg., Kodama et al. 1998), we measure the deviations from the color- $\sigma$  and the  $Mg_2 - \sigma$  relations (solid lines in Fig. 3) for each galaxy, and plotted them against the X-ray extent ( $E_X$ ) in Fig. 4. The raw values of  $S_N$  are re-plotted in the bottom panel. There is no clear trend that any of the optical quantities scale with the X-ray extent. Our result is consistent with White & Sarazin (1991) who found no correlation between the excess of X-ray luminosity for a given optical luminosity and the residual from the scaling relations in  $U - V$  color and  $Mg_2$  index.

To test the above results statistically, we calculate the mean deviations in four colors, the mean deviations in  $Mg_2$  index, and the mean  $S_N$  for the X-ray extended galaxies and the X-ray compact ones separately. The results are summarized in Table 1. The standard deviation within each galaxy category is also given as a measure of internal scatter. Since NGC 1399 and NGC 4486 have significantly larger  $S_N$  values, we excluded these two cD galaxies in calculating the average and the scatter of  $S_N$  for the X-ray extended galaxies. We applied Welch's

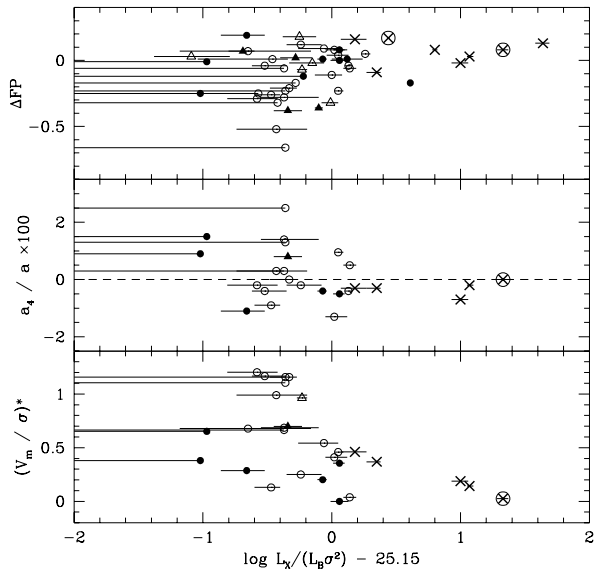


Fig. 5. Deviation from the Fundamental Plane ( $\Delta$  FP), boxy/disky index ( $a_4/a$ ), and velocity anisotropy index  $(V_m/\sigma)^*$  (from top to bottom) are plotted against the X-ray extent defined as  $E_X = \log L_X / (L_B \sigma^2) - 25.15$ . Typical errors for  $(a_4/a \times 100)$  and  $(V_m/\sigma)^*$  are 0.25 and 10%, respectively. Horizontal error-bars correspond to two sigma errors in  $L_X$ . Crosses indicate the X-ray extended galaxies, and those surrounded by big circles are the cD galaxies. The galaxies in cluster environment are shown by filled symbols, while those in the field or in small groups are shown by open symbols. Ellipticals are indicated by circles, while S0's are indicated by triangles.

non-parametric statistical test and found that none of these optical quantities show significant difference between the X-ray extended galaxies and the compact ones. The probability of the difference is always smaller than 90 per cent, and the hypothesis that we draw both samples from the same parent group cannot be rejected.

If a difference of more than 0.078 in  $U - V$  or 0.023 in  $Mg_2$  would have been present between the two groups, it should have been detected at the significance level in this statistical test. This corresponds to the difference in stellar populations of only  $\Delta \log Z = 0.1$  or  $\Delta \log T = 0.15$  for old galaxies (Kodama & Arimoto 1997). Therefore the stellar populations of the early-type galaxies should be homogeneous below this level despite the variety of X-ray extent. The above upper limit for the metallicity difference is rather small compared to the expected difference if the galaxies with the same stellar mass form in various potential depth. We will discuss this point in § 4.

We also plot the deviation from the fundamental plane,  $\Delta$ FP, in the top panel of Fig. 5 as a function of  $E_X$ .  $\Delta$ FP is a measure of the difference of the dynamical mass-to-light ratio from that of the ‘normal’ early-type galaxies with the same dynamical mass (Prugniel & Simien 1996). This indicates the deviations in stellar populations and/or dynamical mass including dark matter. A positive value of  $\Delta$ FP corresponds to a larger mass-to-light ratio. The X-ray extended galaxies generally have a high  $\Delta$ FP, while the X-ray compact ones show a considerable spread towards lower values. Since we have found that the stellar populations are quite homogeneous against  $E_X$ , the above result is indicative of the presence of more dark matter in the X-ray extended galaxies, as expected.

Finally, we compare the isophotal shape and the velocity

anisotropy against the X-ray properties. We first use the  $a_4/a$  index, where  $a_4$  is the fourth cosine coefficient of the Fourier expansion of the deviations from a pure ellipse and  $a$  is the semi-major axis of the isophote (Bender & Möllenhoff 1987). A positive value of  $a_4/a$  means a disk-like isophote, while a negative value corresponds to a box-shaped isophote. The other index,  $V_m/\sigma$  is a ratio between maximum rotation velocity ( $V_m$ ) and central velocity dispersion ( $\sigma$ ), which is transformed to the anisotropy index by taking into account the ellipticity ( $\epsilon$ ):

$$(V_m/\sigma)^* = (V_m/\sigma) / \sqrt{\epsilon/(1-\epsilon)}, \quad (2)$$

following Bender (1988). There are clear trends that the X-ray extended galaxies have a negative  $a_4/a$  and small  $(V_m/\sigma)^*$  with relatively small scatters. These effects should partly come from the dependence of  $a_4/a$  and  $(V_m/\sigma)^*$  on galaxy luminosity (Bender 1988, Bender et al. 1989), because the X-ray extended galaxies are generally bright. However, it is notable that all of the X-ray extended galaxies have boxy shapes and weak rotations. These findings are similar to what Bender (1988) and Bender et al. (1989) found; i.e.,  $a_4/a$  index correlates with the X-ray luminosity excess that comes from the surrounding hot gas halos and also with the velocity anisotropy. Some attempts have been made to understand this kinematical dichotomy of elliptical galaxies in the context of galaxy-galaxy merging using dynamical simulations (Bekki & Shioya 1997; Bruckert et al. 1999). Bruckert et al. (1999) showed that major mergers produced boxy ellipticals with anisotropic velocity, while minor mergers produced the disk-like ones. Considering together that the X-ray extended galaxies are located at the local density peaks, they are possibly the products of major mergers.

After all, although the clear dichotomy in X-ray properties correlates with the isophotal shape and the velocity structure of galaxies, the stellar populations and globular cluster properties are still found to be quite homogeneous.

#### 4. DISCUSSION

We estimate how much metallicity difference is expected between the X-ray extended galaxies and the X-ray compact ones at a given stellar mass (or  $\sigma$ ) if the dichotomy of the potential structure has already been established at the time of star formation. The hydrostatic equilibrium for the ISM gives the galaxy potential of

$$\Phi \propto T \left( \frac{\log \rho}{\log r} + \frac{\log T}{\log r} \right), \quad (3)$$

where  $\rho$  is the density of matters including the dark matter. Since the density gradient  $\log \rho / \log r$  should not differ much between the two galaxy categories (X-ray extended and the X-ray compact ones) within optical radius, and the ISM temperature gradient  $\log T / \log r$  is negligible compared to the density gradient (Forman, Jones & Tucker 1985; Trinchieri et al. 1994; Boute & Canizares 1994), the potential  $\phi$  approximately scales with the ISM temperature  $T$ . Given that there is a factor of 2 difference in  $T$  within  $4 r_e$  between the two galaxy categories for a given  $\sigma$  (§ 2), the X-ray extended galaxies could have experienced twice as many supernova explosions and recycled twice as much metals into the same amount of stars before the gas is expelled. Therefore we could expect that the mean stellar metallicity of the X-ray extended galaxies is twice as high as that of the X-ray compact ones for a given  $\sigma$ . This big difference in metallicity should have been detected in the statistical test in § 3, if present. As opposed to what we expect, however, we do not detect any significant difference in stellar populations between the two. This means that the potential

TABLE 1

DIFFERENCE OF THE INDICES BETWEEN THE X-RAY EXTENDED GALAXIES AND THE X-RAY COMPACT ONES.

Index	X-ray compact	X-ray extended	probability of the difference
$\Delta(U-V)_{e,0}$	$0.00 \pm 0.07$	$-0.04 \pm 0.05$	<90 %
$\Delta(B-V)_{e,0}$	$0.00 \pm 0.03$	$-0.01 \pm 0.02$	<80 %
$\Delta(V-R)_{e,0}$	$0.00 \pm 0.01$	$-0.01 \pm 0.02$	<80 %
$\Delta(V-I)_{e,0}$	$0.00 \pm 0.03$	$-0.01 \pm 0.03$	<50 %
$\Delta \text{Mg}_2$	$0.00 \pm 0.02$	$0.00 \pm 0.02$	<50 %
$S_N$	$3.80 \pm 2.33$	$5.25 \pm 1.73$	<80 %
$\Delta \text{FP}$	$-0.10 \pm 0.19$	$0.07 \pm 0.09$	>99 %
$a_4/a \times 100$	$0.25 \pm 0.98$	$-0.30 \pm 0.26$	>95 %
$(V_m/\sigma)^*$	$0.59 \pm 0.40$	$0.24 \pm 0.18$	>99 %

NOTE.— From top to bottom, the average values are shown for the deviations from the scaling relations of the four colors and  $\text{Mg}_2$  against  $\log \sigma$ ,  $S_N$ , deviation from the fundamental plane, boxy/disky index, and anisotropy index. Standard deviations are given following the  $\pm$  signs as the measure of scatters around the average values. The two cD galaxies, NGC 1399 and NGC 4486, are excluded in calculating the averaged  $S_N$  value and the scatter for the X-ray extended galaxies.

structure of early-type galaxies during the major star formation epoch was quite different from what it is today. Gravitational potential must have been homogeneous. It must not have produced more than only 0.1 dex difference in mean stellar metallicity at a given stellar mass. Later on, after the epoch of major star formation, some galaxies became incorporated into larger scale potentials by infalling into the bottom of the local potential and/or by accumulating the surrounding materials and augmenting their gravitational potential, which eventually resulted in the variety of X-ray extent seen at the present-day.

This picture is consistent with what people have found as to the formation of early-type galaxies: Most of the ‘stars’ in early-type galaxies should form at significantly high redshifts ( $z > 2$ ) (eg., Bower, Lucey & Ellis 1992; Ellis et al. 1997; Stanford, Eisenhardt & Dickinson 1998; Kodama et al. 1998; van Dokkum et al. 1998; Kodama, Bower & Bell 1999), while the ‘mass’ of early-type galaxies can successively grow due to the accretion and/or merging even well below  $z < 2$  in the course of hierarchical assembly (eg., Kauffman 1996; Baugh et al. 1998; Bower, Kodama & Terlevich 1998; van Dokkum et al. 1999).

From our results, we speculate that the chemical abundance of ISM in  $\alpha$ -elements (such as O, Mg, Si, and S which come mainly from SN Type II) should be quite uniform at a fixed stellar mass of the central galaxy regardless of its X-ray extent. The individual potential structure of a galaxy is independent of the larger scale potential and should be similar at the time of major star formation. Davis & White (1996) and Loewenstein et al. (1994) claimed that galaxies with lower ISM temperature or compact X-ray halos tend to have lower chemical abundance of the ISM. However, it is not yet clear whether there is such a correlation for the  $\alpha$ -elements abundance (Matsushita, Makishima & Ohashi 2000). The new X-ray satellite XMM will solve this problem. On the other hand, the contribution from SN Type Ia can be much different because the potential structure would vary at the time of a SN Ia explosion due to the time delay of the explosion (Yoshii, Tsujimoto & Nomoto 1996). The X-ray extended galaxies would have acquired deeper potential wells by then, keep the SNIa ejecta more efficiently and hence show relatively iron enhanced ISM abundance compared to the X-ray

compact ones. This is what we actually observe by ASCA. Although the ISM abundance of the X-ray compact galaxies is still uncertain, if we assume the same  $\alpha$ -element abundance as the X-ray extended systems, the Fe abundance is about a factor of 2 smaller than that of the X-ray extended objects (Matsushita, Makishima & Ohashi 2000).

Considering that the X-ray extended galaxies are sitting in the center of larger scale potential structures and that dynamical friction drives satellite galaxies towards the center, these galaxies are more likely to be produced by galaxy mergers. The fact that the X-ray extended galaxies tend to have boxy shapes and weak rotation might support this hypothesis. If this is really the case, and if a considerable number of new globular clusters form during galaxy mergers as suggested by Zepf & Ashman (1993), we should expect higher  $S_N$  for the X-ray extended galaxies on average. However, there is no significant difference in  $S_N$  except for the cD galaxies. This may imply that, apart from the cD galaxies, the secondary globular clusters do not generally form by recent galaxy mergers, and that most of the globular clusters around the X-ray extended galaxies are likely to form very early when the major star formation takes place in their host galaxies.

## 5. CONCLUSIONS

The stellar population makeup in early-type galaxies does not correlate with their present-day global potential structure. Early-type galaxies form stars at early epoch in their own potential wells independently, and some of the galaxies become incorporated into larger scale potential structures (clusters/groups) later on. This idea naturally explains the homogeneity of the stellar populations despite the variety of X-ray properties.

This work was supported by the Japan Society for the Promotion of Science (JSPS) through its Research Fellowships for Young Scientists. We thank K. Pimblet for carefully reading the paper and polishing up English as well as giving us some useful comments.

## REFERENCES

- Ashman, K. M., & Zepf, S. E., 1998, *Globular Cluster Systems*, Cambridge astrophysics series Vol. 30, (Cambridge University Press; Cambridge)
- Bassino, L. P., Muzzio, J. C., & Rabolli, M., 1994, *ApJ*, 431, 634
- Baugh, C. M., Cole, S., Frenk, C. S., & Lacey, C. G., 1998, *ApJ*, 498, 504
- Bekki, K., & Shioya, Y., 1997, *ApJ*, 478, L17
- Bender, R., 1988, *A&A*, 193, L7
- Bender, R., & Möllenhoff, C., 1987, *A&A*, 177, 71
- Bender, R., Surma, P., Döbereiner, S., Möllenhoff, C., & Madejsky, R., 1989, *A&A*, 217, 35
- Boute, D. A., & Canizares, C. R., 1994, *ApJ*, 427, 86
- Bower, R. G., Lucey, J. R., & Ellis, R. S., 1992, *MNRAS*, 254
- Bower, R. G., Kodama, T., & Terlevich, A., 1998, *MNRAS*, 299, 1193
- Burkert, A., Naab, T., 1999, in 'Galaxy Dynamics: from the Early Universe to the Present', eds., F. Combes, G. A. Mamon, & V. Charmandaris, ASP Conference Series, in press
- Burstein, D., Davies, R. L., Dressler, A., Faber, S. M., Lynden-Bell, D., Terlevich, R., Wegner, G., 1988, in *Towards Understanding Galaxies at Large Redshift*, ed. R. G., Kron & A. Renzini (Dordrecht: Kluwer).
- Buta, R. J., & Williams, K. L., 1995, *AJ*, 109, 543
- Ciotti, L., Pellegrini, S., Renzini, A., & D'Ercole, A., 1991, *ApJ*, 376, 380
- Côté, P., Marzke, R. O., & West, M. J., 1998, *ApJ*, 501, 554
- Davis, D. S., & White, R. E., 1996, *ApJ*, 470, L35
- Ellis, R. S., Smail, I., Dressler, A., Couch, W. J., Oemler, A., Butcher, H., & Sharples, R. M., 1997, *ApJ*, 483, 582
- Faber, S. M., Wegner, G., Burstein, D., Davies, R. L., Dressler, A., Lynden-Bell, D., Terlevich, R., 1989, *ApJS*, 69, 763
- Forman, W., Jones, C., & Tucker, W., 1985, *ApJ*, 293, 102
- Holtzman, J. A., et al., 1996, *AJ*, 112, 416
- Kauffmann, G., 1996, *MNRAS*, 281, 487
- Kodama, T., & Arimoto N., 1997, *A&A*, 320, 41
- Kodama, T., Arimoto, N., Barger, A. J., & Aragón-Salamanca, A. 1998, *A&A*, 334, 99
- Kodama, T., Bower, R. G., & Bell, E. F., 1999, *MNRAS*, 306, 561
- Larson, M., 1994, *MNRAS*, 169, 229
- Loewenstein, M., et al., 1994, *ApJ*, 436, L75
- Matsushita, K., 1997, Ph.D. thesis, University of Tokyo
- Matsushita, K., Makishima, K., Ikebe, Y., Rokutanda, E., Yamasaki, N., & Ohashi, T., 1998, *ApJ*, 499, L13
- Matsushita, K., 2000, *ApJ*, submitted (M2000)
- Matsushita, K., Makishima, K., & Ohashi, T., 2000, *PASJ*, submitted
- Prugniel, P., & Simien, F., 1996, *A&A*, 309, 749
- Richer, H. B., Crabtree, D. R., Fabian, A. C., & Lin, D. N. C., 1993, *AJ*, 105, 877
- Rieke, G. H. & Lebofsky, M. J., 1985, *ApJ*, 288, 618
- Schweizer F., & Seitzer, P., 1992, *AJ*, 104, 1039
- Stanford, S. A., Eisenhardt, P. R. M., & Dickinson, M., 1998, *ApJ*, 492, 461
- Trinchieri, G., Kim, D.-W., Fabbiano, G., & Canizares, C. R., 1994, *ApJ*, 428, 555
- Tully, R. B., 1988, *Nearby Galaxies Catalogue*, Cambridge University Press
- de Vaucouleurs, G., de Vaucouleurs, A., Corwin, H. G., Buta, R. J., Paturel, G., & Fouqué, P., 1991, *Third Reference Catalogue of Bright Galaxies (Springer;Berlin) (RC3)*
- van Dokkum, P. G., Franx, M., Kelson, D. D., & Illingworth, G. D., 1998, *ApJ*, 504, L17
- van Dokkum, P. G., Franx, M., Fabricant, D., Kelson, D. D., & Illingworth, G. D., 1999, *ApJ*, 520, L95
- White, R. E., & Sarazin, C. L., 1991, *ApJ*, 367, 476
- Yoshii, Y., Tsujimoto, T., & Nomoto, K., 1996, *ApJ*, 462, 266
- Zepf, S. E., & Ashman, K. M., 1993, *MNRAS*, 264, 611